Inorganic Chemistry

Article

Exceptional Photochemical Stability of the Co−C Bond of Alkynyl Cobalamins, Potential Antivitamins B₁₂ and Core Elements of B₁₂-Based Biological Vectors

Elvin V. Salerno, Nicholas A. Miller, Arkaprabha Konar, Robert Salchner, Christoph Kieninger, Klaus Wurst, Kenneth G. Spears, Bernhard Kräutler,* and Roseanne J. Sension*

Cite This: *Inorg. Chem.* 2020, 59, 6422−6431

Read Online

ACCESS | 📊 Metrics & More | 📰 Article Recommendations | 🔵 Supporting Information

ABSTRACT: Alkynylcorrinoids are a class of organometallic B₁₂ derivatives, recently rediscovered for use as antivitamins B₁₂ and as core components of B₁₂-based biological vectors. They feature exceptional photochemical and thermal stability of their characteristic extra-short Co−C bond. We describe here the synthesis and structure of 3-hydroxypropynylcobalamin (HOPryCbl) and photochemical experiments with HOPryCbl, as well as of the related alkynylcobalamins: phenylethynylcobalamin and difluoro-phenylethynylcobalamin. Ultrafast spectroscopic studies of the excited state dynamics and mechanism for ground state recovery demonstrate that the Co−C bond of alkynylcobalamins is stable, with the Co−N bond and ring deformations mediating internal conversion and ground state recovery within 100 ps. These studies provide insights required for the rational design of photostable or photolabile B₁₂-based cellular vectors.
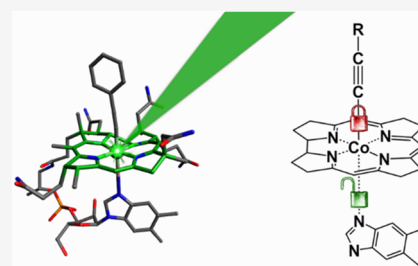
INTRODUCTION

Vitamin B₁₂ (cyanocobalamin, CNCbl) and other cobalamins (Cbl's) are natural cobalt corrinoids, having a 5′,6′-dimethylbenzimidazole (DMB) ligand tethered to the "lower" side of the corrin moiety. "Upper" axial ligands (cyano, 5′-deoxyadenosyl and methyl groups) complete the set of six Co(III)-coordinated ligand atoms in CNCbl, coenzyme B₁₂ (adenosylcobalamin, AdoCbl), and methylcobalamin (MeCbl; Figure 1).[1−3] A weak Co−C bond is a biologically crucial property of the organometallic enzyme cofactors AdoCbl and MeCbl,[4−7] which also function as the specific high-affinity ligands in the gene-regulatory B₁₂ riboswitches.[8−10] The B₁₂ cofactors and synthetic organometallic B₁₂ derivatives were typically found to be light-sensitive due to rapid photolytic cleavage of their Co−C bond.[11−14] Nature has exploited this feature effectively, and AdoCbl functions as a light receptor controlling gene expression (e.g., in CarH).[15,16] The B₁₂ community has, in fact, always been fascinated by the photochemical properties of the typically red colored vitamin B₁₂ derivatives.[12−14,17,18]

Organometallic B₁₂ derivatives have found use as reagents and catalysts exploiting the unique reactivity of their weak (Co−C) bond.[19−22] Recently, significant efforts have been devoted to the design of B₁₂ derivatives as medicinal and biological probes.[23−28] The Cbl-derived so-called antivitamins B₁₂ are organometallic Cbl's that are taken up by Cbl-transport proteins but are inert to transformation into biologically active B₁₂ cofactors.[29−32] Antivitamins B₁₂ impair the bioavailability of B₁₂ by filling the physical but not functional space of cobalamins in humans and other mammals,[33] as well as in

other B₁₂-dependent organisms.[34,35] Hence, thermal and photochemical stability has been a desirable property of the originally designed organometallic Cbl-derived antivitamins B₁₂.[29] However, thermally stable but photolabile (or "photoconditional") antivitamin B₁₂ derivatives have also raised interest,[36] as their use promises to allow the spatiotemporal control of B₁₂ bioactivity and also to deliver spatiotemporally localized therapeutics. Cbl-based "photoconditional" antivitamins B₁₂ should be photolabile, whereby the removal of the "upper" axial (Co_β-R) ligand by light would uncage B₁₂ bioactivity.[29] Likewise, in some B₁₂-based biological vectors, the light induced release of the attached drug may be an attractive property.[28,37,38]

The rational design of either photostable or photolabile antivitamins B₁₂, and of B₁₂-based cellular vectors, requires insights into the elementary photochemistry of such B₁₂ derivatives, based on an understanding of the factors that promote or inhibit cleavage of their (Co_β−C) bond in the excited electronic state manifold.[39] We have recently reported on 4-ethylphenylcobalamin (EtPhCbl) as a photolabile organometallic aryl-type antivitamin B₁₂[30] and studied the remarkable, quantum-inefficient light-induced cleavage of its
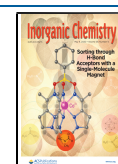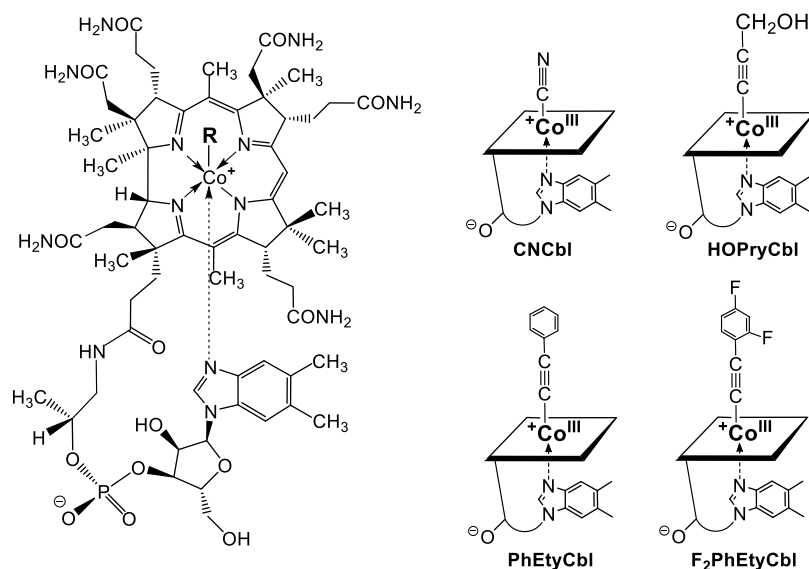
Figure 1. Structural formulas of vitamin B$_{12}$ derivatives. Left: Formulas of B$_{12}$ cofactors. In coenzyme B$_{12}$ (AdoCbl), R = 5′-deoxyadenosyl and, in methylcobalamin (MeCbl), R = CH$_3$. Right: Symbolic formulas of the four Cbl compounds discussed in this work: vitamin B$_{12}$ (cyanocobalamin, CNCbl) and the Co$_\beta$-alkynyl-Cbl's 3-HO-propynylcobalamin (HOPryCbl), phenylethynylcobalamin (PhEtyCbl), and 4,6-difluorophenylethynylcobalamin (F$_2$PhEtyCbl).

Co−C$_{sp2}$ bond.[36] The more recent presentation of the alkynylcobalamin 2-phenylethynyl-cobalamin (PhEtyCbl), with a Co−C≡C−R "upper" axial ligand, as a robust and apparently photostable potential antivitamin B$_{12}$ (see Figure 1)[31,32] has prompted a photochemical investigation of PhEtyCbl.[36] The exceptional stability of PhEtyCbl against thermolytic and photolytic cleavage of its organometallic bond[31] has inspired biological and biomedical applications of a range of alkynyl Cbl's.[27,32,40,41] Hence, we became interested in the crucial electronic properties of alkynyl Cbl's that are instrumental in strengthening their Co$_\beta$−C bond, inhibiting photoinduced Co$_\beta$−C bond dissociation by enhancing internal conversion and repopulation of the ground state.

Recent TD-DFT calculations[39] also explored the photostability of PhEtyCbl. Its photoexcitation is predicted to populate a local minimum on the electronically excited state near the Franck−Condon geometry followed by barrier crossing to a global minimum involving dissociation of the Co−N$_{DMB}$ bond. Optical excitation is dominated by a corrin ring π → π* transition, but the HOMO → LUMO transition of both Co−N$_{DMB}$ base-on PhEtyCbl and the corresponding base-off compound involves delocalization over the phenyl and ethynyl groups. The excited state electronic configuration following internal conversion and structural relaxation is best described as (π_{corrin} π_{PhEty}).[39] Subsequent return to the ground state is mediated by corrin ring distortion in a Co−N$_{DMB}$ base-off configuration. For PhEtyCbl, there is not an energetically favorable path for photolysis; rather, internal conversion is the significantly preferred photophysical event.

In the context of our photochemical studies with alkynyl-Cbl's, photostable CNCbl has become a relevant model, as the basic pattern of its Co$_\beta$−C bonding relates to that of the Co$_\beta$-alkynyl-Cbl's.[31] Spectroscopic measurements[42−47] and theoretical simulations[48,49] on CNCbl suggest that the fast internal conversion of CNCbl (ca. 6 ps at room temperature in aqueous solution) is mediated through axial bond expansion involving both Co−C and Co−N$_{DMB}$, allowing access to a seam between the ground S$_0$ and excited S$_1$ potential energy

surfaces. A recent transient X-ray absorption near edge structure (XANES) measurement of the excited state structure of the related alkynyl cobalamin, 2-[2,4-difluorophenyl]-ethynylcobalamin (F$_2$PhEtyCbl),[32] is consistent with elongation, but not dissociation of the Co−N$_{DMB}$ bond in the excited state accompanied by little or no change in the Co$_\beta$−C bond.[50] The differences between the properties of alkynyl Cbl's and CNCbl suggest that the excited state structure and the mechanism for efficient internal conversion and ground state recovery is not simply related to the presence of an sp-hybridized carbon bonded as the upper axial ligand to the cobalt center.

These observations raise the question of the role of the ethynyl and phenyl group in controlling the photochemical properties of alkynyl cobalamins. Specifically, what effect does ring substitution or removal of the phenyl ring altogether have on the excited state dynamics and photochemistry? Here, we present ultrafast transient absorption studies that examine the photophysics and ground state recovery of the alkynyl cobalamins, F$_2$PhEtyCbl and 3-hydroxypropynyl cobalamin (HOPryCbl). The results are compared with those obtained in prior work on PhEtyCbl and CNCbl to present a more complete picture of Co−C≡C−R excited state dynamics and the mechanism for internal conversion to the ground state.

■ EXPERIMENTAL METHODS

Syntheses and Characterization of Alkynyl-Cbl's. PhEtyCbl[31] and F$_2$PhEtyCbl[32] were synthesized as published. Crystalline HOPryCbl was prepared here from aquocobalamin (H$_2$OCbl) in 60% yield using the formate reduction methodology developed with PhEtyCbl[31] (see Supporting Information for details). Previously, the synthesis of HOPryCbl in 52% yield was achieved using CNCbl, Cu(I) acetate, and 3-hydroxypropyne.[40] HOPryCbl is fully characterized here, based on UV/vis, CD, IR, mass, and ¹H NMR spectra, as displayed in the Supporting Information. By means of homonuclear and heteronuclear NMR spectroscopy, the structure of HOPryCbl in aqueous solution was secured (see Supporting Information). Single crystals of HOPryCbl were grown for an X-ray analysis that provided detailed structural insights into the bonding pattern around the cobalt center of HOPryCbl.

Scheme 1. Synthesis of HOPryCbl from H₂OCbl by Formate Reduction and Alkynylation with 3-Hydroxypropynyl Iodide
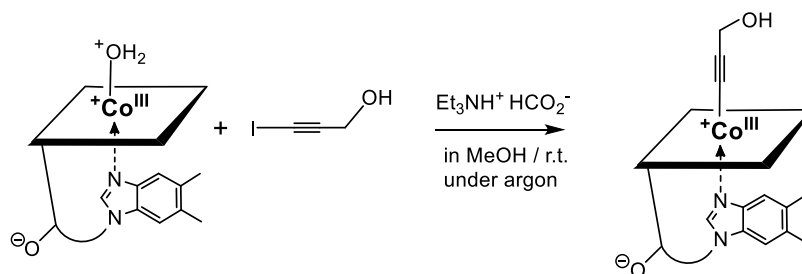
Transient Absorption Measurements. Ultrafast transient absorption measurements were performed using three distinct Ti:sapphire laser systems. All systems amplify ca. 808 to 816 nm femtosecond pulses in 1 kHz regenerative or multipass amplifier systems to 1 mJ with a duration < 100 fs. Excitation pulses between 404 and 408 nm were produced by second harmonic generation. Visible excitation pulses ca. 540 to 550 nm were produced using a noncollinear optical parametric amplifier (NOPA). Cobalamin samples were measured at a concentration of 1 mg/mL in a 1 mm path length cuvette. Temperature control was achieved using a Neslab water bath to immerse the sample reservoir and to cool or heat the sample cell holder. Temperature measurement used a thermocouple inserted into the sample near the sample cell holder. See the Supporting Information for additional details.

Materials and Spectroscopy. See the Supporting Information.

■ RESULTS

Synthetic, Spectroscopic, and X-ray Crystallographic Studies. Crystalline 3-hydroxpropynylcobalamin (HOPryCbl) was prepared here in 60% yield from aquocobalamin (H₂OCbl) via a recently developed methodology using 3-hydroxypropynyl iodide and formate as reducing agents[31] (see Scheme 1 and the Supporting Information for details). An aqueous solution of HOPryCbl featured a UV/vis spectrum with pronounced maxima at 368 and 553 nm, as is typical of alkynyl-Cbl's (see Figure 2).[31,32,40] In the IR spectrum, the
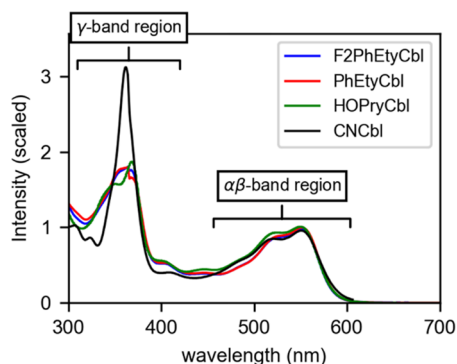

Figure 2. UV−visible absorption spectra of the cobalamins investigated in this work. The spectra are scaled to the same intensity at the ca. 550 nm peak of the α-band.

signal at 2135 cm⁻¹ indicated a C≡C stretch stronger by about 20 cm⁻¹ than in PhEtyCbl and about 16 cm⁻¹ stronger than in 3-hydroxy-propyne itself (see Table S1). Homonuclear and heteronuclear NMR spectra established its solution structure and confirmed NMR spectroscopic data reported earlier.[40]

From a concentrated solution of HOPryCbl in methanol, single crystals (orthorhombic space group $P2_12_12_1$) separated

out, suitable for X-ray analysis (Figure 3 and Supporting Information). The crystal structure analysis confirmed the NMR-derived data and furnished detailed insights into the bonding pattern around the cobalt center. Hence, HOPryCbl exhibits a basic structure closely related to those of the alkynyl-Cbl's PhEtyCbl[31,40] and of F₂PhEtyCbl.[32] However, the length of the C≡C bond of HOPryCbl of 1.19 Å is slightly shorter by 0.02 Å than the one of PhEtyCbl, qualitatively consistent with the also noted higher C≡C stretching frequency. The remarkably short organometallic $Co_\beta−C$ and $Co−N_{DMB}$ bonds in HOPryCbl (of 1.89 and 2.09 Å, respectively) indicate strong σ-bonding and considerable π back bonding interactions between the d^6 Co(III) center and both of the unsaturated axial ligands, consistent with partial double bond character of the two axial bonds to the cobalt center. Such bonding features are characteristics of the crystal structures not only of alkynyl-Cbl's[31,32,51] but of CNCbl,[52,53] as well.

Solutions of HOPryCbl in DMSO were stable to exposure to daylight (see Figure S9) and underwent only slow decomposition at 100 °C (half-life of roughly 20 h), producing insignificant amounts of aquocobalamin as a product of the cleavage of the Co−C bond, but a variety of other (nonidentified) decomposition products (see Supporting Information). In the solid, HOPryCbl has been reported to decompose at >190 °C.[40] Solutions of PhEtyCbl and F₂PhEtyCbl in DMSO showed insignificant thermal decomposition after 3 days at 100 °C,[31,32] a consistent consequence of the proposed strong Co−C bond of alkynyl-Cbl's.[31]

Photochemical Studies. Vitamin B₁₂ (CNCbl) and the three alkynyl-Cbl's have similar UV−visible spectra (Figure 2) in the αβ-band region and a prominent γ-band transition in the ultraviolet, although the latter is broader in the alkynyl cobalamins than the γ-band of CNCbl. Ultrafast transient absorption measurements were performed with excitation at 540 or 550 nm, into the lowest allowed excited electronic state at or near the excited state maximum or with excitation at 408 nm placing an additional 6000 cm⁻¹ of excess energy into the photoexcited molecule.

3-Hydroxypropynylcobalamin (HOPryCbl). The excited state dynamics and internal conversion of HOPryCbl were examined as a function of solvent and temperature. The excitation wavelength was 408 or 540 nm with transient absorption spectra essentially independent of excitation wavelength after the first several hundred femtoseconds. Here, we are focused on the excited state dynamics and ground state recovery on time scales >1 ps. A transient spectrum obtained in water at 23 °C using 540 nm excitation is plotted in Figure 4.

The data were fit to a sum of exponential decay components and a Gaussian instrument response function (IRF) to gather rate constants for three events. The data in Figure 4 are well
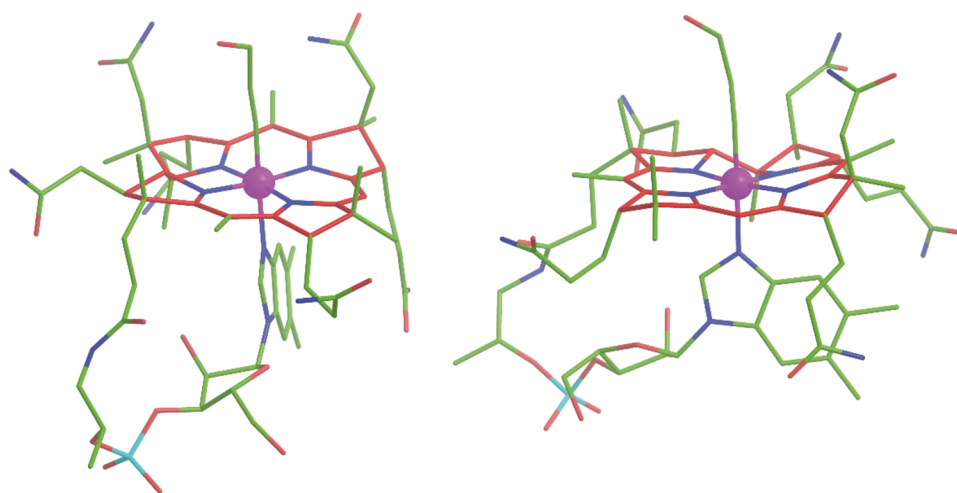
Figure 3. Stick model of the structure of HOPryCbl in the crystal from X-ray analysis, depicted in two orientations, highlighting the corrin core and the axial ligands (color code of the corrin core: Co, pink sphere; C, red; N, blue; color code of the axial ligands and the periphery: C, green; N, blue; O, red; P, turquoise). For details, such as disorder in the terminal position of the 3-hydroxypropynyl ligand and location of H-bonded water molecules, see the Supporting Information).
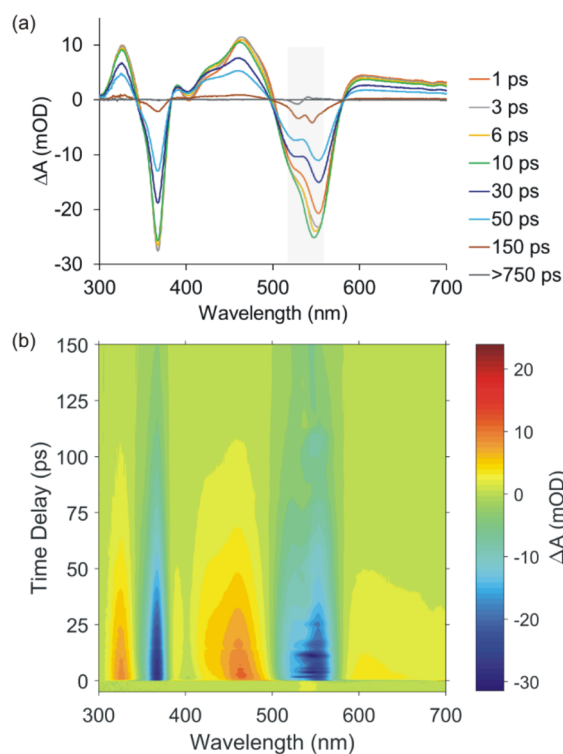

Figure 4. Transient absorption signal obtained following excitation of HOPryCbl at 540 nm. The sample temperature was held at 23 °C. The data set extends to delay times of 900 ps. (a) Lineouts at select time delays. The transient signal decays to baseline on a ca. 55 ps time scale leaving only baseline for long delays indicating the absence of a long-lived photoproduct. The gray shaded box indicates the region influenced by the subtraction of the signal resulting from scatter of the excitation pulse. (b) Surface plot of the time-dependent difference spectrum of the electronically excited cobalamin.
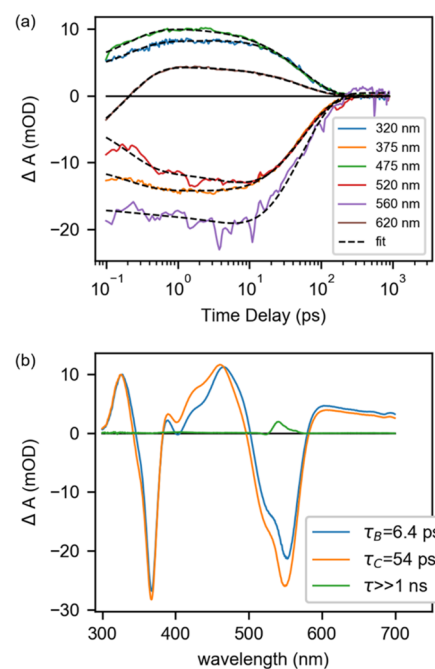

Figure 5. Global fit to transient absorption of HOPryCbl following 540 nm excitation. (a) Comparison of kinetic traces and the exponential fit at several key wavelengths as indicated. (b) Species associated difference spectra (SADS) for the intermediates observed after the first picosecond as determined from the global fit to the data. The plots are labeled with the lifetime of each component. The residual at long times ($\gg$ 1 ns) is zero except for the influence of pump scatter around 540 nm.

AdoCbl.[54] This component depends on excitation wavelength and does not impact the question of photochemical stability, thus it will not be considered further here. The decay associated difference spectra (DADS) represent the amplitudes of each decay component as a function of wavelength. DADS for excitation at 408 and 540 nm excitation are plotted in Figures S11 and S12 for comparison. Given a model for the excited state dynamics, the DADS can be used to produce the species associated difference spectra (SADS). We assume a

characterized using one ultrashort component, τ_A = 200 fs, and two picosecond components, τ_B = 6.4 ps and τ_C = 55 ps, as illustrated at selected wavelengths in Figure 5a. The femtosecond component reports on motion out of the initial Franck−Condon excited state as reported recently for

Table 1. Rate Constants (and Lifetimes) for the Excited States B and C of HOPryCbl As a Function of Solvent and Temperature

solvent	temperature (°C)	η (cp)	ε^a	λ_{exc} (nm)	k_B ps^{-1} (τ_B ps)^g	k_C ps^{-1} (τ_C ps)^h
water	11			540	0.090 (11)	0.0142 (70)
water	19	1.027^b	80.1	408	0.169 (5.9)	0.0163 (61)
water	23			540	0.156 (6.4)	0.0184 (54)
water	42			540	0.178 (5.6)	0.0278 (36)
water	56			540	0.214 (4.7)	0.0321 (31)
water	73			540	0.265 (3.8)	0.0364 (27)
ethanol	8			408	0.134 (7.5)	0.0095 (105)
ethanol	21	1.185^c	24.6	408	0.189 (5.3)	0.0124 (81)
ethanol	36			408	0.305 (3.3)	0.0154 (65)
ethanol	55			408	0.448 (2.2)	0.0210 (48)
ethanol	75			408	0.584 (1.7)	0.0272 (37)
methanol	19	0.586^c	32.7	408	0.254 (3.9)	0.0143 (70)
2-butanol	20	3.74^d	20	408	0.375 (2.7)	0.0072 (139)
3:1 EG/H$_2$O	20	8.07^e	46^f	408	0.139 (7.2)	0.0072 (139)
ethylene glycol	19	22.3^e	37	408	0.040 (25)	0.0060 (167)

^{a}Dielectric constants at 20 °C[57] unless otherwise indicated. ^{b}Ref 55. ^{c}Viscosity at 20 °C.[56] ^{d}Ref 58. ^{e}Ref 59. ^{f}Dielectric constant at 25 °C.[60] ^{g}The average error bars on k_B are ±0.01. ^{h}The error bars on k_C were estimated conservatively based on upper and lower limits for potential fits to the data and are included in Figure 7. These range from ±0.001 at low temperatures to ±0.0025 at the highest temperatures.

sequential model, $GS \xrightarrow{h\nu} A \xrightarrow{\tau_A} B \xrightarrow{\tau_B} C \xrightarrow{\tau_C} GS$ to produce the SADS, and the derivation of relevant formulas is reported elsewhere.[36] The SADS for 23 °C and 540 nm excitation are plotted in Figure 5b.

The nature of the reaction coordinate for internal conversion may be further probed by varying the solvent. The effect of solvent polarity on excited state dynamics will probe charge migration or charge separation during excited state rearrangement. The effect of solvent viscosity on excited state dynamics probes the degree to which significant overall expansion or contraction takes place. The viscosity and polarity dependence of the excited state lifetime of HOPryCbl was investigated at room temperature (ca. 19−21 °C) in a variety of solvents. These data are summarized in Figure S13 and in Table 1.

In comparison with CNCbl, where a strong polarity dependence is observed,[43,44] there is a lack of a clear trend with polarity for HOPryCbl, suggesting that excited state charge migration plays little role in the reaction coordinate for internal conversion. Only a general trend with viscosity is present (see Figure S14); the internal conversion is faster in the low viscosity solvents (η around 1 mPa s) than the high viscosity solvents ($\eta \geq 4$ mPa s). In the absence of a strong dependence of lifetime on viscosity or polarity, an Arrhenius analysis of the temperature dependence will provide insight into the excited state barrier for internal conversion that is not complicated by temperature dependent properties of the solvent. Transient absorption measurements of HOPryCbl in water were performed at 11 °C, 42 °C, 56 °C, and 73 °C. The results are summarized in Table 1 and Figure S15. The lifetimes of the picosecond components, τ_B and τ_C, decrease with temperature consistent with a barrier crossing mechanism for population decay. Temperature dependent measurements were also performed in ethanol for temperatures ranging from 8 to 75 °C (see Figures S16 and S17). Water and ethanol have similar viscosities (1.002 and 1.185 cP at 20 °C),[55,56] but disparate dielectric constants (80.1 and 24.6 at 25 °C).[57]

The longest-lived excited state, C, is associated with internal conversion to the ground state and thus is our major target of further analysis. SADS for state C in water across varying temperatures are plotted in Figure 6. The broad excited state
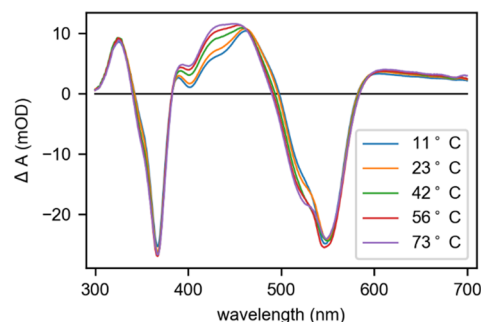

Figure 6. SADS for the stable excited state of HOPryCbl as a function of temperature. The blue shift of the excited state absorption between 400 and 470 nm increases with temperature.

absorption to the red of the photobleach around 550 nm is common to many cobalamins. The peak around 460 nm reflects a blue shift of the $\alpha\beta$ band in the excited state, consistent with an increase in the axial bond lengths (see Discussion). This absorption is strongly dependent on temperature. The temperature dependent variation around 420−450 nm is significantly smaller in ethanol (see Figure S17).

The temperature dependent rates for internal conversion to the ground state (k_C) were fit to the Arrhenius equation: ln k_C = $-E_a/RT$ + ln A_h where the activation barrier E_a and the exponential prefactor A_h are assumed to be independent of temperature. The results are plotted in Figure 7. A weighted linear regression taking into account the error in each rate constant was used to determine the values for E_a. The activation barrier is independent of solvent, suggesting that the solvent dependence of the rate for internal conversion is controlled by the prefactor A_h. Unlike CNCbl,[44] the barrier for internal conversion in HOPryCbl is independent of solvent polarity. The barrier is also identical within experimental error to the barrier reported earlier for PhEtyCbl in water as shown in Figure 7.[36]

2-[2,4-Difluorophenyl]ethynyl-Cobalamin. To complement the studies of PhEtyCbl[36] and HOPryCbl, transient absorption measurements were performed on 2-[2,4-
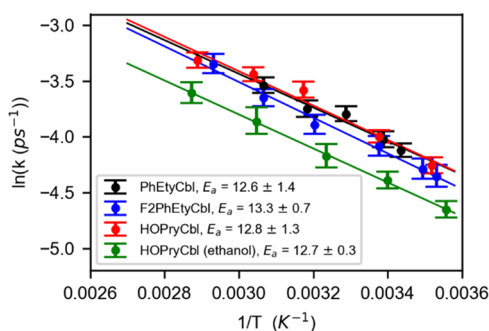
Figure 7. Arrhenius plots of $\ln(k)$ vs $1/T$ for the internal conversion to the ground state. The barrier is the same within experimental error for all three alkynyl Cbl's.

difluorophenyl]ethynyl-Cbl (F$_2$PhEtyCbl, see Figure 1). Measurements were performed using excitation at 408 and 550 nm. Data obtained using 550 nm excitation are plotted in Figure 8. The transient spectra observed for F$_2$PhEtyCbl are
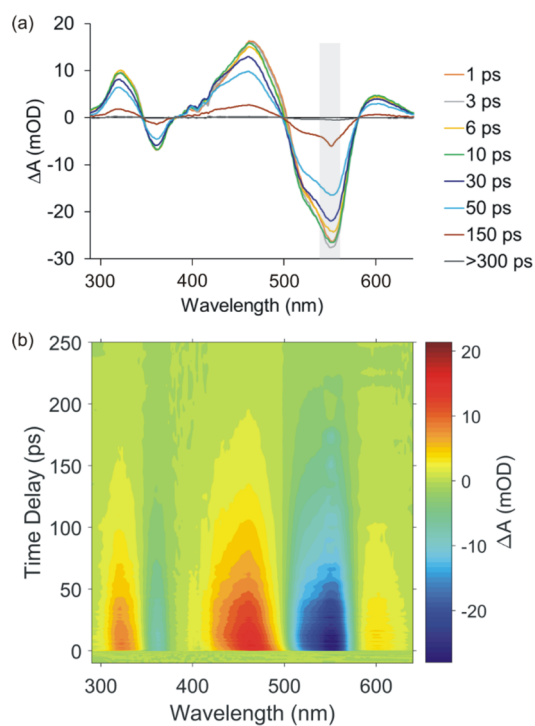

Figure 8. Transient absorption signal obtained following excitation of F$_2$PhEtyCbl at 550 nm. The sample temperature was held at 10−13 °C. The data set extends to delay times of 450 ps. (a) Lineouts at select time delays. The transient signal decays to zero on a ca. 75 ps time scale leaving only a baseline for long delays. The gray shaded box indicates the region influenced by the subtraction of the signal resulting from scatter of the excitation pulse. (b) Surface plot of the time-dependent difference spectrum of the electronically excited cobalamin.

independent of excitation wavelength for times greater than 0.5 ps. The transient spectra are similar to those observed for PhEtyCbl and HOPryCbl although the lifetimes vary.

The transient absorption scan was fit to a model consisting of three exponential decay components (Figure S18). The fastest time constant, ca. 0.20 ps, is not considered further here for the reasons given above for HOPryCbl; it is not important in determining the excited state internal conversion process.

The longer two rate constants are summarized in Table 2. These measurements were repeated at temperatures ranging

Table 2. Rate and Time Constants for the Excited States of F$_2$PhEtyCbl and PhEtyCbl in Water As a Function of Temperature

temperature (°C)	λ_{exc} (nm)	k_B (ps^{-1})[a]	τ_B ps	k_C (ps^{-1})[b]	τ_C ps
		F$_2$PhEtyCbl			
RT (ca. 18)	406	0.145	6.9	0.0139	72.5
10	550	0.102	9.8	0.0128	78.0
13	550	0.087	11.5	0.0137	72.9
23	550	0.148	6.8	0.0168	59.4
39	550	0.127	7.9	0.0204	49.0
53	550	0.167	6.0	0.0260	38.5
68	550	0.187	5.3	0.0352	28.4
		PhEtyCbl[8]			
18	406	0.117	8.5	0.0162	61.7
22	550	0.117	8.6	0.0179	55.9
31	550	0.128	7.8	0.0225	44.5
41	550	0.159	6.3	0.0236	42.4
53	550	0.151	6.6	0.0291	34.4

[a]The average error bars on k_B are ±0.01. [b]The error bars on k_C were estimated conservatively based on upper and lower limits for potential fits to the data and are included in Figure 7. These range from ±0.001 at low temperatures to ±0.003 at the highest temperatures.

from 10° to 68 °C. Both PhEtyCbl and F$_2$PhEtyCbl exhibit an excited state absorption that blue-shifts with temperature, although the spectral changes are more subtle than observed for HOPryCbl (see Figure S19). An analysis of the temperature dependence of the rate constant for internal conversion using the Arrhenius equation leads to an activation barrier of 13.3 ± 0.7 kJ/mol, similar to the barriers determined for PhEtyCbl and HOPryCbl (see Figure 7). This barrier is determined primarily by the alkynyl linkage rather than the identity of the organic group attached to the ethynyl carbon.

■ **DISCUSSION**

The alkynyl cobalamins studied here feature a thermally and photochemically stable Co$_\beta$−C$_{sp}$ bond,[31,32,36,40,50,51] in contrast to the ready heat- or light-induced cleavage of the weak Co$_\beta$−C bond in the two biologically active coenzymes, MeCbl and AdoCbl.[12−14] The excited state of alkynyl Cbl's undergoes internal conversion to the ground state on a time scale < 100 ps without cleavage of the strong Co$_\beta$−C$_{sp}$ bond. CNCbl can be considered the prototypical cobalamin species with an sp-hybridized carbon bonded as the upper axial ligand to the cobalt center. Like the alkynyl Cbl's, CNCbl is both thermally and photochemically stable (photolysis quantum yield ≤ 10^{-4} in solution, dependent on pH and likely through a triplet mechanism).[61,62] Unlike the alkynyl Cbl's, which are (potential) antivitamins B$_{12}$,[31,32] CNCbl functions as a vitamin, as it is reduced *in vivo* by the enzyme CblC to cob(II)alamin which is a metabolic precursor of active B$_{12}$ cofactors.[63] The results presented above and discussed below demonstrate that the properties of alkynyl Cbl's that are instrumental in inhibiting photoinduced Co$_\beta$−C bond dissociation differ significantly from the properties instrumental in inhibiting photodissociation and enhancing internal conversion in CNCbl.

Transient absorption studies of CNCbl suggested that the excited state structure is characterized by elongated axial

bonds.[42,43,47] This expectation was confirmed by theoretical simulations[48,49] and by measurements of the time-resolved X-ray absorption near edge structure (XANES) following photoexcitation.[45,46] Comparisons of the transient polarized XANES measurements with theoretically predicted excited state structures demonstrate that the Co−N$_{DMB}$ bond of CNCbl expands by ca. 10% (∼0.2 Å), while the Co$_\beta$−C bond expansion is 15% to 19% (∼0.3 to 0.35 Å).[46,48,49] Ultrafast IR measurements indicate that the stretching frequency of the C≡N triple bond in CNCbl shifts 20 to 30 cm^{-1} to lower frequency in the excited state.[43,47] The bonding of CN$^-$ to a transition metal cation results in transfer of electron density from a σ_{CN}^* orbital of the cyano group to the metal and d−π* back-bonding into the CN ligand.[53] Thus, a decrease in the strength of the Co−C bond is correlated with increased σ* character and a decrease in the strength of the C≡N bond, lowering its vibrational frequency.

The excited state lifetime of CNCbl (ca. 6 to 20 ps) is largely independent of solvent viscosity but strongly dependent on solvent polarity.[43,44] Solvent polarity modifies the excited state barrier for internal conversion according to the phenomenological equation $E_a(\varepsilon) = E_a^1 - \alpha(\varepsilon - 1)$ where E_a^1 is the activation barrier for internal conversion in a vacuum ($\varepsilon = 1$) and α is a parameter determined from a fit to the experimental data.[44] For CNCbl, $\alpha \approx 0.047$. The barrier for the gas phase molecule is determined as 12.5 ± 0.5 kJ/mol, and the activation barrier in water at room temperature is estimated to be 8.8 kJ/mol. We hypothesize that the polarity dependence of the barrier for internal conversion to the ground state is a consequence of the explicit polarity of the C≡N bond. The polarity of the solvent modifies the influence of this bond on the Co$_\beta$−C bond and thus the crossing with the ground state along the Co$_\beta$−C coordinate. The extension of both the Co$_\beta$−C and Co−N$_{DMB}$ bonds in the excited state provides an effective pathway for rapid internal conversion to the ground state without cleavage of the Co$_\beta$−C bond.

In contrast, a transient XANES measurement on F$_2$PhEtyCbl demonstrates little change in the Co$_\beta$−C bond,[50] in good qualitative agreement with TD-DFT calculations on PhEtyCbl.[39] The Co$_\beta$−C bond is "locked" near the ground state bond length. In addition, the C≡C bond is nonpolar and insensitive to solvent polarity, eliminating an important mechanism for the potential influence of environment on internal conversion. The dominant structural change in the excited electronic state of alkynl Cbl's is in the Co−N$_{DMB}$ bond, which lengthens significantly in the excited state. Further insight into the flexibility of the Co−N$_{DMB}$ bond can be obtained from the excited state optical spectrum. Figure 9 shows ground and estimated excited state spectra for CNCbl, PhEtyCbl, HOPryCbl, and F$_2$PhEtyCbl in water. The general spectral features for each of these species in the ground state are very similar in the $\alpha\beta$-band region with two prominent peaks and a shoulder. There is also a pronounced γ-band at ca. 360 nm, although the width and intensity vary.

The estimated excited state spectra for HOPryCbl and F$_2$PhEtyCbl are determined by adding the ground state spectrum back into the SADS as described previously for CNCbl and PhEtyCbl.[36,42] In the excited state, all four compounds exhibit a blue-shifted $\alpha\beta$-band characteristic of extension of one or both axial bonds.[43,45,64] For comparison, (photoinduced) homolytic cleavage of the Co$_\beta$−C bond of AdoCbl, MeCbl, and related organometallic Cbl's furnishes cob(II)alamin and results in a blue shift of the $\alpha\beta$ band to 470
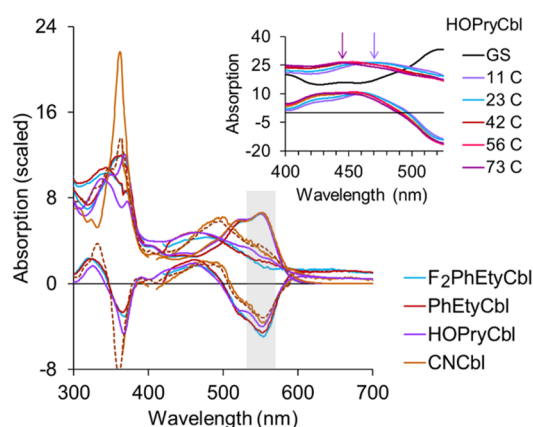

Figure 9. Ground and estimated excited state absorption spectra of the four molecules discussed here. The color code is the same for the difference, ground state, and excited state spectra. The data are scaled to the ground state $\alpha\beta$-band absorption at 550 nm. Two data sets are shown for CNCbl, one with ca. 400 nm excitation (solid lines, 365 to 700 nm) and one with 550 nm excitation (dashed lines, 300 to 590 nm). The HOPryCbl data were obtained using 550 nm excitation, while F$_2$PhEtyCbl and PhEtyCbl data were obtained with ca. 408 nm excitation. The gray shaded area is perturbed by pump scatter when the excitation wavelength is ca. 550 nm. The inset shows the temperature dependence of the excited state absorption peak for HOPryCbl. This peak shifts from ca. 470 nm at 11 °C to 445 nm at 73 °C.

nm.[13,44] At pH < 3, the DMB base of alkylcobalamins (e.g., AdoCbl and MeCbl) becomes protonated accompanied by a transition from their so-called base-on configuration to their protonated base-off form (see Figure S20). The base-on to base-off transition results in a blue shift of the $\alpha\beta$-band absorption to ca. 460 nm.[5,65] A pK_a of 3.7 has likewise been measured for the protonated base-off form of the arylcobalamin 4-ethylphenylcobalamin.[30] F$_2$PhEtyCbl[32] and related alkynyl-Cbl's[31,40] require more acidic environments to be transformed into their protonated base-off forms, which can be detected by a characteristic blue shift of the $\alpha\beta$ band by roughly 30 nm. However, at low pH, alkynyl-Cbl's are not stable and decompose to aquocobalamin. Half-life times of roughly 2 and 5 h, respectively, have been observed at pH 1 and room temperature for F$_2$PhEtyCbl and for HOPryCbl (see Supporting Information).

The excited state spectra for the alkynyl-Cbl's are similar to each other with a peak at ca. 465 nm at room temperature consistent with elongation or dissociation of the Co−C$_{DMB}$ bond. CNCbl is different: the blue shift is smaller, and the absorption band is stronger. The differences are consistent with distinct excited state structures for CNCbl and the alkynyl cobalamins and with a larger role for Co−N$_{DMB}$ elongation in the latter. The pronounced temperature dependence of the excited state $\alpha\beta$-band absorption of HOPryCbl in water, and smaller dependence for HOPryCbl in ethanol and PhEtyCbl and F$_2$PhEtyCbl in water, is consistent with a shallow potential for the Co−N$_{DMB}$ bond and a variation in the average bond length with temperature. Taken together with the excited state XANES data on F$_2$PhEtyCbl, these results demonstrate that the Co−N$_{DMB}$ bond is weakened in the excited state with a shallow potential such that the degree of lengthening or dissociation of this bond is dependent on temperature.

The alkynyl ligand stabilizes the cobalamin against photolytic cleavage of the Co$_\beta$−C bond and modifies the mechanism

for internal conversion and ground state recovery from that observed in the related vitamin B_{12}. In CNCbl, the barrier for internal conversion to the ground state is strongly dependent on solvent polarity and involves elongation of both axial bonds. In contrast, the weak dependence of the excited state lifetime of alkynyl cobalamins on solvent properties and the similarity of the barrier for ground state recovery for all three alkynyl cobalamins studied (see Figure 7) are consistent with return to the ground state mediated by corrin ring distortion from a structure with an elongated Co–C_{DMB} bond as predicted in theoretical calculations of the excited state of PhEtyCbl, although the calculated barriers are much higher than the experimental results.[39]

CONCLUSIONS

Alkynylcobalamins have recently been explored as robust vitamin B_{12} analogues,[31,32,40,51] useful as potential antivitamins B_{12}[32] and as versatile organometallic B_{12}-based biological vectors.[27] Alkynyl-Cbl's feature unique structural properties and an exceptional thermal and photochemical stability of their Co_{β}–C_{sp} bond. The excited state of alkynyl-Cbl's undergoes rapid internal conversion to the ground state (on a time scale < 100 ps) without cleavage of the strong Co_{β}–C_{sp} bond. Comparison with results on CNCbl demonstrates that the ethynyl π orbitals interacting with the cobalt-corrin moiety provide a mechanism to further stabilize and shorten the Co_{β}–C_{sp} bond. These interactions also prevail in the excited singlet state and inhibit elongation and internal conversion or bond dissociation pathways requiring bond elongation. The excited state structure and the mechanism for efficient ground state recovery is not only due to the presence of an sp-hybridized carbon bonded as the upper axial ligand to the cobalt center. All three of the alkynyl-Cbl's studied here exhibit similar time scales and barriers for internal conversion to the ground state. This is consistent with a deactivation mechanism largely decoupled from the particular R group of the Co–C≡C–R axial ligand and dominated by corrin ring distortion from an excited state minimum and significant elongation of the Co–N_{DMB} bond, as predicted in theoretical simulations.[39]

As delineated here, the design of light-sensitive alkynyl Cbl's as photoconditional antivitamins B_{12} appears challenging. It would require analogues, in which the R group in the Co–C≡C–R unit would strongly reduce the π-bonding influence of the π_{Ety} orbitals in the lowest excited electronic state, enhancing the readiness for cleavage of the Co_{β}–C_{sp} bond. Theoretical calculations along these lines may provide insights helpful in directing the design of such compounds. However, the complete inertness of alkynyl-Cbl's against cleavage by light provides a solid basis for the design and use of such organometallic B_{12} derivatives as photostable antivitamins B_{12}[29] as versatile "Trojan Horses" carrying drugs into cells and organisms,[27] and in a range of other biological applications.[40]

ASSOCIATED CONTENT

Ⓢ Supporting Information

The Supporting Information is available free of charge at https://pubs.acs.org/doi/10.1021/acs.inorgchem.0c00453.

> Detailed description of the synthesis procedures, complete spectroscopic and crystallographic information (including the crystal structure deposition code), as well as additional photophysical data figures; additional transient absorption data figures for HOPryCbl and F₂PhEtyCbl including plots of decay associated difference spectra and the polarity and viscosity dependence of the HOPryCbl excited state lifetime (PDF)

Accession Codes

CCDC 1964021 contains the supplementary crystallographic data for this paper. These data can be obtained free of charge via www.ccdc.cam.ac.uk/data_request/cif, or by emailing data_request@ccdc.cam.ac.uk, or by contacting The Cambridge Crystallographic Data Centre, 12 Union Road, Cambridge CB2 1EZ, UK; fax: +44 1223 336033.

AUTHOR INFORMATION

Corresponding Authors

Bernhard Kräutler − *Institute of Organic Chemistry and Center for Molecular Biosciences, University of Innsbruck, A-6020 Innsbruck, Austria;* ⓞ orcid.org/0000-0002-2222-0587; Phone: +43-676-8725-52000; Email: Bernhard.kraeutler@uibk.ac.at

Roseanne J. Sension − *Department of Chemistry, Department of Physics, and Biophysics, University of Michigan, Ann Arbor, Michigan 48109-1055, United States;* ⓞ orcid.org/0000-0001-6758-0132; Phone: 734-763-6074; Email: rsension@umich.edu

Authors

Elvin V. Salerno − *Department of Chemistry, University of Michigan, Ann Arbor, Michigan 48109-1055, United States*

Nicholas A. Miller − *Department of Chemistry, University of Michigan, Ann Arbor, Michigan 48109-1055, United States;* ⓞ orcid.org/0000-0002-9146-5414

Arkaprabha Konar − *Department of Physics, University of Michigan, Ann Arbor, Michigan 48109-1040, United States;* ⓞ orcid.org/0000-0001-6546-4111

Robert Salchner − *Institute of Organic Chemistry and Center for Molecular Biosciences, University of Innsbruck, A-6020 Innsbruck, Austria*

Christoph Kieninger − *Institute of Organic Chemistry and Center for Molecular Biosciences, University of Innsbruck, A-6020 Innsbruck, Austria*

Klaus Wurst − *Institute of General, Inorganic and Theoretical Chemistry, University of Innsbruck, A-6020 Innsbruck, Austria*

Kenneth G. Spears − *Department of Chemistry, University of Michigan, Ann Arbor, Michigan 48109-1055, United States*

Complete contact information is available at:
https://pubs.acs.org/10.1021/acs.inorgchem.0c00453

Notes

The authors declare no competing financial interest.

REFERENCES

(1) Hodgkin, D. C. X-ray analysis of complicated molecules. *Science* **1965**, *150*, 979−988.

(2) *Vitamin B$_{12}$ and B$_{12}$-Proteins*; Kräutler, B., Arigoni, D., Golding, B. T., Eds.; John Wiley VCH: Weinheim, 1998.

(3) *Chemistry and Biochemistry of B$_{12}$*; Banerjee, R., Ed.; John Wiley & Sons: New York, 1999.

(4) Banerjee, R.; Ragsdale, S. W. The many faces of vitamin B$_{12}$: Catalysis by cobalamin-dependent enzymes. *Annu. Rev. Biochem.* **2003**, *72*, 209−247.

(5) Gruber, K.; Puffer, B.; Kräutler, B. Vitamin B$_{12}$-derivatives - enzyme cofactors and ligands of proteins and nucleic acids. *Chem. Soc. Rev.* **2011**, *40*, 4346−4363.

(6) Buckel, W.; Golding, B. T. Radical enzymes in anaerobes. *Annu. Rev. Microbiol.* **2006**, *60*, 27−49.

(7) Zhang, Q.; van der Donk, W.; Liu, W. Radical-mediated enzymatic methylation: A tale of two SAMS. *Acc. Chem. Res.* **2012**, *45*, 555.

(8) Nahvi, A.; Barrick, J. E.; Breaker, R. R. Coenzyme B$_{12}$ riboswitches are widespread genetic control elements in prokaryotes. *Nucleic Acids Res.* **2004**, *32*, 143−150.

(9) Peselis, A.; Serganov, A. Structural insights into ligand binding and gene expression control by an adenosylcobalamin riboswitch. *Nat. Struct. Mol. Biol.* **2012**, *19*, 1182−1184.

(10) Johnson, J. E.; Reyes, F. E.; Polaski, J. T.; Batey, R. T. B$_{12}$ cofactors directly stabilize an mRNA regulatory switch. *Nature* **2012**, *492*, 133−137.

(11) Taylor, R. T.; Smucker, L.; Hanna, M. L.; Gill, J. Aerobic photolysis of alkylcobalamins - quantum yields and light-action spectra. *Arch. Biochem. Biophys.* **1973**, *156*, 521−533.

(12) Jones, A. R. The photochemistry and photobiology of vitamin B$_{12}$. *Photochem. & Photobiol. Sci.* **2017**, *16*, 820−834.

(13) Rury, A. S.; Wiley, T. E.; Sension, R. J. Energy cascades, excited state dynamics, and photochemistry in cob(III)alamins and ferric porphyrins. *Acc. Chem. Res.* **2015**, *48*, 860−867.

(14) Toda, M. J.; Lodowski, P.; Al Mamun, A.; Jaworska, M.; Kozlowski, P. M. Photolytic properties of the biologically active forms of vitamin B$_{12}$. *Coord. Chem. Rev.* **2019**, *385*, 20−43.

(15) Padmanabhan, S.; Jost, M.; Drennan, C. L.; Elias-Arnanz, M. A new facet of vitamin B$_{12}$: Gene regulation by cobalamin-based photoreceptors. *Annu. Rev. Biochem.* **2017**, *86*, 485−514.

(16) Jost, M.; Fernandez-Zapata, J.; Polanco, M. C.; Ortiz-Guerrero, J. M.; Chen, P. Y.-T.; Kang, G.; Padmanabhan, S.; Elias-Arnanz, M.; Drennan, C. L. Structural basis for gene regulation by a B$_{12}$-dependent photoreceptor. *Nature* **2015**, *526*, 536−541.

(17) Pratt, J. M. *Inorganic Chemistry of Vitamin B$_{12}$*; Academic Press: New York, 1972.

(18) Giannotti, C. In *B$_{12}$*; Dolphin, D., Ed.; Wiley & Sons: New York, 1982; Vol. I, pp 393−430.

(19) Scheffold, R.; Rytz, G.; Walder, L.; Orlinski, R.; Chilmonczyk, Z. Formation of (C-C)bonds catalyzed by vitamin-B$_{12}$. *Pure Appl. Chem.* **1983**, *55*, 1791−1797.

(20) Hisaeda, Y.; Tahara, K.; Shimakoshi, H.; Masuko, T. Bioinspired catalytic reactions with vitamin B$_{12}$ derivative and photosensitizers. *Pure Appl. Chem.* **2013**, *85*, 1415−1426.

(21) Giedyk, M.; Goliszewska, K.; Gryko, D. Vitamin B$_{12}$ catalysed reactions. *Chem. Soc. Rev.* **2015**, *44*, 3391−3404.

(22) Shell, T. A.; Shell, J. R.; Rodgers, L.; Lawrence, D. S. Tunable visible and near-IR photoactivaton of light-responsive compounds by using fluorophores as light-capturing antennas. *Angew. Chem., Int. Ed.* **2014**, *53*, 875−878.

(23) Lee, M.; Grissom, C. B. Design, synthesis, and characterization of fluorescent cobalamin analogues with high quantum efficiencies. *Org. Lett.* **2009**, *11*, 2499−2502.

(24) Zelder, F.; Alberto, R. In *Handbook of Porphyrin Science*; Kadish, K. M., Smith, K. M., Guilard, R., Ed.; World Scientific, 2012; Vol. 25, pp 84−132.

(25) Rownicki, M.; Wojciechowska, M.; Wierzba, A. J.; Czarnecki, J.; Bartosik, D.; Gryko, D.; Trylska, J. Vitamin B$_{12}$ as a carrier of peptide nucleic acid (PNA) into bacterial cells. *Sci. Rep.* **2017**, *7*, 7644.

(26) Giedyk, M.; Jackowska, A.; Równicki, M.; Kolanowska, M.; Trylska, J.; Gryko, D. Vitamin B$_{12}$ transports modified RNA into E. coli and S. Typhimurium cells. *Chem. Commun.* **2019**, *55*, 763−766.

(27) Rossier, J.; Nasiri Sovari, S.; Pavic, A.; Vojnovic, S.; Stringer, T.; Battig, S.; Smith, G. S.; Nikodinovic-Runic, J.; Zobi, F. Antiplasmodial activity and in vivo bio-distribution of chloroquine molecules released with a 4-(4-ethynylphenyl)-triazole moiety from organometallo-cobalamins. *Molecules* **2019**, *24*, 2310.

(28) Shell, T. A.; Lawrence, D. S. Vitamin B$_{12}$: A tunable, long wavelength, light-responsive platform for launching therapeutic agents. *Acc. Chem. Res.* **2015**, *48*, 2866−2874.

(29) Kräutler, B. Antivitamins B$_{12}$ - a structure- and reactivity-based concept. *Chem. - Eur. J.* **2015**, *21*, 11280−11287.

(30) Ruetz, M.; Gherasim, C.; Fedosov, S. N.; Gruber, K.; Banerjee, R.; Kräutler, B. Radical synthesis opens access to organometallic aryl-cobaltcorrins - 4-ethylphenyl-cobalamin, a potential "antivitamin B$_{12}$." *Angew. Chem., Int. Ed.* **2013**, *52*, 2606−2610.

(31) Ruetz, M.; Salchner, R.; Wurst, K.; Fedosov, S.; Kräutler, B. Phenylethynylcobalamin: A light-stable and thermolysis-resistant organometallic vitamin B$_{12}$ derivative prepared by radical synthesis. *Angew. Chem., Int. Ed.* **2013**, *52*, 11406−11409.

(32) Ruetz, M.; Shanmuganathan, A.; Gherasim, C.; Karasik, A.; Salchner, R.; Kieninger, C.; Wurst, K.; Banerjee, R.; Koutmos, M.; Krautler, B. Antivitamin B$_{12}$ inhibition of the human B$_{12}$-processing enzyme CblC: Crystal structure of an inactive ternary complex with glutathione as the cosubstrate. *Angew. Chem., Int. Ed.* **2017**, *56*, 7387−7392.

(33) Mutti, E.; Ruetz, M.; Birn, H.; Kräutler, B.; Nexo, E. 4-ethylphenyl-cobalamin impairs tissue uptake of vitamin B$_{12}$ and causes vitamin B$_{12}$ deficiency in mice. *PLoS One* **2013**, *8*, e75312.

(34) Guzzo, M. B.; Nguyen, H. T.; Pham, T. H.; Wyszczelska-Rokiel, M.; Jakubowski, H.; Wolff, K. A.; Ogwang, S.; Timpona, J. L.; Gogula, S.; Jacobs, M. R.; Ruetz, M.; Kräutler, B.; Jacobsen, D. W.; Zhang, G.-F.; Nguyen, L. Methylfolate trap promotes bacterial thymineless death by sulfa drugs. *PLoS Pathog.* **2016**, *12*, e1005949.

(35) Widner, F. J.; Lawrence, A. D.; Deery, E.; Heldt, D.; Frank, S.; Gruber, K.; Wurst, K.; Warren, M. J.; Kräutler, B. Total synthesis, structure, and biological activity of adenosylrhodibalamin, the non-natural rhodium homologue of coenzyme B$_{12}$. *Angew. Chem., Int. Ed.* **2016**, *55*, 11281−11286.

(36) Miller, N. A.; Wiley, T. E.; Spears, K. G.; Ruetz, M.; Kieninger, C.; Kräutler, B.; Sension, R. J. Toward the design of photoresponsive conditional antivitamins B$_{12}$: A transient absorption study of an arylcobalamin and an alkynylcobalamin. *J. Am. Chem. Soc.* **2016**, *138*, 14250−14256.

(37) Hunger, M.; Mutti, E.; Rieder, A.; Enders, B.; Nexo, E.; Kräutler, B. Organometallic B$_{12}$-DNA-conjugate: Synthesis, structure analysis and studies of binding to human B$_{12}$-transporter proteins. *Chem. - Eur. J.* **2014**, *20*, 13103−13107.

(38) Hughes, R. M.; Marvin, C. M.; Rodgers, Z. L.; Ding, S.; Oien, N. P.; Smith, W. J.; Lawrence, D. S. Phototriggered secretion of membrane compartmentalized bioactive agents. *Angew. Chem.* **2016**, *128*, 16314−16317.

(39) Lodowski, P.; Toda, M. J.; Ciura, K.; Jaworska, M.; Kozlowski, P. M. Photolytic properties of antivitamins B$_{12}$. *Inorg. Chem.* **2018**, *57*, 7838−7850.

(40) Chrominski, M.; Lewalska, A.; Karczewski, M.; Gryko, D. Vitamin B$_{12}$ derivatives for orthogonal functionalization. *J. Org. Chem.* **2014**, *79*, 7532−7542.

(41) Jakubaszek, M.; Rossier, J.; Karges, J.; Delasoie, J.; Goud, B.; Gasser, G.; Zobi, F. Evaluation of the potential of cobalamin derivatives bearing Ru(II) polypyridyl complexes as photosensitizers for photodynamic therapy. *Helv. Chim. Acta* **2019**, *102*, 8.

(42) Wiley, T. E.; Arruda, B. C.; Miller, N. A.; Lenard, M.; Sension, R. J. Excited electronic states and internal conversion in cyanocobalamin. *Chin. Chem. Lett.* **2015**, *26*, 439−443.

(43) Shiang, J. J.; Cole, A. G.; Sension, R. J.; Hang, K.; Weng, Y. X.; Trommel, J. S.; Marzilli, L. G.; Lian, T. Q. Ultrafast excited-state

dynamics in vitamin B_{12} and related cob(III)alamins. *J. Am. Chem. Soc.* **2006**, *128*, 801−808.

(44) Harris, D. A.; Stickrath, A. B.; Carroll, E. C.; Sension, R. J. Influence of environment on the electronic structure of Cob(III)-alamins: Time-resolved absorption studies of the S_1 state spectrum and dynamics. *J. Am. Chem. Soc.* **2007**, *129*, 7578−7585.

(45) Miller, N. A.; Deb, A.; Alonso-Mori, R.; Garabato, B. D.; Glownia, J. M.; Kiefer, L. M.; Koralek, J.; Sikorski, M.; Spears, K. G.; Wiley, T. E.; Zhu, D. L.; Kozlowski, P. M.; Kubarych, K. J.; Penner-Hahn, J. E.; Sension, R. J. Polarized XANES monitors femtosecond structural evolution of photoexcited vitamin B_{12}. *J. Am. Chem. Soc.* **2017**, *139*, 1894−1899.

(46) Miller, N. A.; Deb, A.; Alonso-Mori, R.; Glownia, J. M.; Kiefer, L. M.; Konar, A.; Michocki, L. B.; Sikorski, M.; Sofferman, D. L.; Song, S.; Toda, M. J.; Wiley, T. E.; Zhu, D. L.; Kozlowski, P. M.; Kubarych, K. J.; Penner-Hahn, J. E.; Sension, R. J. Ultrafast X-ray absorption near edge structure reveals ballistic excited state structural dynamics. *J. Phys. Chem. A* **2018**, *122*, 4963−4971.

(47) Jones, A. R.; Russell, H. J.; Greetham, G. M.; Towrie, M.; Hay, S.; Scrutton, N. S. Ultrafast infrared spectral fingerprints of vitamin B_{12} and related cobalamins. *J. Phys. Chem. A* **2012**, *116*, 5586−5594.

(48) Lodowski, P.; Jaworska, M.; Andruniow, T.; Garabato, B. D.; Kozlowski, P. M. Mechanism of the S_1 excited state internal conversion in vitamin B_{12}. *Phys. Chem. Chem. Phys.* **2014**, *16*, 18675−18679.

(49) Lodowski, P.; Jaworska, M.; Kornobis, K.; Andruniow, T.; Kozlowski, P. M. Electronic and structural properties of low-lying excited states of vitamin B_{12}. *J. Phys. Chem. B* **2011**, *115*, 13304−13319.

(50) Miller, N. A.; Michocki, L. B.; Alonso-Mori, R.; Britz, A.; Deb, A.; DePonte, D. P.; Glownia, J. M.; Kaneshiro, A. K.; Kieninger, C.; Koralek, J.; Meadows, J. H.; van Driel, T. B.; Krautler, B.; Kubarych, K. J.; Penner-Hahn, J. E.; Sension, R. J. Antivitamins B_{12} in a microdrop: The excited-state structure of a precious sample using transient polarized X-ray absorption near-edge structure. *J. Phys. Chem. Lett.* **2019**, *10*, 5484−5489.

(51) Chrominski, M.; Lewalska, A.; Gryko, D. Reduction-free synthesis of stable acetylide cobalamins. *Chem. Commun.* **2013**, *49*, 11406−11408.

(52) Kräutler, B.; Konrat, R.; Stupperich, E.; Färber, G.; Gruber, K.; Kratky, C. Direct evidence for the conformational deformation of the corrin ring by the nucleotide base in vitamin-B_{12} - synthesis and solution spectroscopic and crystal-structure analysis of co$_\beta$-cyano-imidazolyl-cobamide. *Inorg. Chem.* **1994**, *33*, 4128−4139.

(53) Mebs, S.; Henn, J.; Dittrich, B.; Paulmann, C.; Luger, P. Electron densities of three B_{12} vitamins. *J. Phys. Chem. A* **2009**, *113*, 8366−8378.

(54) Miller, N. A.; Michocki, L. B.; Konar, A.; Alonso-Mori, R.; Deb, A.; Glownia, J. M.; Sofferman, D. L.; Song, S.; Kozlowski, P. M.; Kubarych, K. J.; Penner-Hahn, J. E.; Sension, R. J. Ultrafast XANES monitors sequential structural evolution in photoexcited coenzyme B_{12}. *J. Phys. Chem. B* **2020**, *124*, 199−209.

(55) Huber, M. L.; Perkins, R. A.; Laesecke, A.; Friend, D. G.; Sengers, J. V.; Assael, M. J.; Metaxa, I. N.; Vogel, E.; Mareš, R.; Miyagawa, K. New international formulation for the viscosity of H_2O. *J. Phys. Chem. Ref. Data* **2009**, *38*, 101−125.

(56) Tu, C.-H.; Lee, S.-L.; Peng, I. H. Excess volumes and viscosities of binary mixtures of aliphatic alcohols (C1−C4) with nitromethane. *J. Chem. Eng. Data* **2001**, *46*, 151−155.

(57) *CRC Handbook of Chemistry and Physics*, 99th ed.; Rumble, J. R., Ed.; CRC Press: Boca Raton, FL, 2019.

(58) Spasojević, V. D.; Djordjević, B. D.; Šerbanović, S. P.; Radović, I. R.; Kijevčanin, M. L. Densities, refractive indices, viscosities, and spectroscopic study of 1-amino-2-propanol + 1-butanol and + 2-butanol solutions at (288.15 to 333.15) k. *J. Chem. Eng. Data* **2014**, *59*, 1817−1829.

(59) Sun, T. F.; Teja, A. S. Density, viscosity, and thermal conductivity of aqueous ethylene, diethylene, and triethylene glycol mixtures between 290 and 450 K. *J. Chem. Eng. Data* **2003**, *48*, 198−202.

(60) Uosaki, Y.; Kitaura, S.; Moriyoshi, T. Static relative permittivities of water + ethane-1,2-diol and water + propane-1,2,3-triol under pressures up to 300 mpa at 298.15 K. *J. Chem. Eng. Data* **2006**, *51*, 423−429.

(61) Vogler, A.; Hirschmann, R.; Otto, H.; Kunkely, H. Photo-chemistry of biologically important transition metal complexes. I. Cyanocobalamin and related corrin complexes of rhodium(III). *Ber. Bunsenges. Phys. Chem.* **1976**, *80*, 420−424.

(62) Ahmad, I.; Hussain, W.; Fareedi, A. A. Photolysis of cyanocobalamin in aqueous-solution. *J. Pharm. Biomed. Anal.* **1992**, *10*, 9−15.

(63) Banerjee, R.; Gherasim, C.; Padovani, D. The tinker, tailor, soldier in intracellular B_{12} trafficking. *Curr. Opin. Chem. Biol.* **2009**, *13*, 484−491.

(64) Yoder, L. M.; Cole, A. G.; Walker, L. A., II; Sension, R. J. Time-resolved spectroscopic studies of B_{12} coenzymes: Influence of solvent on the photolysis of adenosylcobalamin. *J. Phys. Chem. B* **2001**, *105*, 12180−12188.

(65) Peng, J. A.; Tang, K. C.; McLoughlin, K.; Yang, Y.; Forgach, D.; Sension, R. J. Ultrafast excited-state dynamics and photolysis in base-off B_{12} coenzymes and analogues: Absence of the trans-nitrogenous ligand opens a channel for rapid nonradiative decay. *J. Phys. Chem. B* **2010**, *114*, 12398−12405.